Tech Science Press

Longitudinal Vibration Analysis of Elastically Coupled Nanorods System with General Boundary Supports

Deshui Xu, Jingtao Du* and Yuhao Zhao

College of Power and Energy Engineering, Harbin Engineering University, Harbin, China.

*Corresponding Author: Jingtao Du. Email: dujingtao@hrbeu.edu.cn.

Abstract: In this paper, an accurate series solution for the longitudinal vibration analysis of elastically coupled nanorods system is established, in which artificial springs are introduced to simulate such general coupling and boundary conditions. Energy formulation is derived for the description of axial dynamics of multiple coupled nanorods based on Eringen nonlocal elasticity. For each nanorod component, its longitudinal vibration displacement function is invariantly assumed as the superposition of Fourier series and boundary smoothed supplementary polynomials, with the aim to make all the spatial differential sufficiently continuous across each rod. All the unknown coefficients are determined in conjunction with Rayleigh-Ritz procedure to solve a standard eigenvalue matrix. Numerical results are presented for the particular cases of two-nanorod and three-nanorod systems to demonstrate the correctness and effectiveness of the proposed model. Excellent agreements can be repeatedly observed in comparison with those from other approaches available in literature. Based on the model established, influence of elastic boundary and coupling conditions on the longitudinal modal characteristics of multiple nanorods system is investigated and addressed. This work can provide an efficient energy-based modeling framework for longitudinal vibration analysis of elastically connected nanorod system with complicated boundary conditions.

Keywords: Longitudinal vibration; nanorods system; elastic boundary and coupling; energy-based method

1 Introduction

With the rapid development of nanotechnology, nanostructures have attracted great attention in various scientific communities, due to their extensive application in micro and nanoscale devices such as nanosensors, nanoactuators, micro and nanoelectro-mechanical devices, nanoopto-mechanical systems [1-3]. In many occasions, an effective and efficient design of such nanostructure system depends on a good understanding on its modal characteristics of such system in small scale. For this reason, a lot of research effort has been devoted to the free vibration analysis of nanostructures, such as nanorings [4], carbon nanotubes [5,6], nanoplates and graphenes [7,8].

For the structural system in such nano-scale, investigation on its dynamic behavior suffers many difficulties in various experiments. In contrast, numerical simulation analysis can serve as an effective way for this purpose, while simulation study based on the traditional continuous theory will not capture the dynamic characteristics well caused by such small-scale effect. With the aim to overcome this issue, Eringen [9] proposed a so-called nonlocal elasticity theory to account for the size effect prominent at nanometer scale, in which the stress at a reference point is assumed as a functional of strain field at every point in continuum. From then on, a lot of research has been carried out based on such theoretical framework for modeling various nanostructures. A general nonlocal beam model was built up for bending, buckling as well as vibration analysis of nanobeams/nanorods [10-14]. Peddieson et al. [15] introduced the nonlocal elasticity theory to nanotechnology, in which they developed a nonlocal Euler-Bernoulli beam model and

then used this theoretical model for deflection analysis of cantilever beam. Ansari and Rouhi [16] investigated the vibration characteristics of single walled carbon nanotubes (SWCNTs) under different boundary conditions using a nonlocal elastic shell model. Lei et al. [17] examined the dynamic characteristics of damped viscoelastic nonlocal beams. Danesh et al. [18] employed the differential quadrature method for axial vibration analysis of tapered nanorod based on nonlocal elasticity theory.

Under certain circumstance, nanostructure is usually subjected to dynamic excitation along the axial direction, and the corresponding design of nanostructure is then to unitize or avoid the longitudinal resonance. Therefore, longitudinal vibration behavior of one-dimensional nanostructure also causes a lot of research attention from some researchers. Aydogdu [19] developed the nonlocal elastic rod model and solved the axial vibration frequencies for clamped-clamped and clamped-free boundary conditions. Kiani [20] obtained the longitudinal vibration frequencies and phase velocities of tapered nanowires via a perturbation technique based on the Fredholm alternative theorem. Guo and Yang [21] employed a modified Wentzel-Brillouin-Kramers (WBK) method to derive the asymptotic solution for axial vibration of general non-uniform nanorods. Xu et al. [22] developed an exact solution for the free longitudinal vibration of nanorod with arbitrary boundary conditions by an improved Fourier series method. Besides the single nanorod case, longitudinal vibration analysis of system consisting multiple nanorods is also investigated in nanostructure community. Murmu and Adhikari [23] carried out the longitudinal vibration analysis of a double nanorod system (DNRS) via the nonlocal elasticity theory. It was assumed that these two nanorods are mechanically coupled through the continuously distributed axial springs between the interfaces. Then, the nonlocal viscoelastic double-nanorod system with Clamped-Clamped (C-C) and Clamped-Free (C-F) boundary conditions is investigated by Karličić et al. [24] and the results are also compared with those calculated from the local double-rod model in the paper of Erol and Gürgöze [25].

As an important structural parameter, boundary condition has a significant influence on modal characteristics of structural system [26]. The current studies on longitudinal vibration analysis of multiple nanorod structure are mainly limited to the classical boundary conditions, such as free and clamped. Actually, due to the inherent microfabrication limitations, these classical boundary conditions are difficult to realize in practical nanostructures, which usually tend to be elastically restrained. Kobrinsky et al. [27] studied mechanical properties of doubly supported silicon-micromachined beams, and they found that support compliance can cause significant effect on the performance of these micromachined devices. Alkharabsheh and Younis [28] examined the dynamic behavior of MEMS arches using a shallow-arch model with rotational and transversal springs at its boundaries. Zhong et al. [29] discussed the non-ideal boundary conditions and the equivalent stiffness for the case of flexible supports in MEMS cantilever-based sensors. In contract, there is little work performed for the multiple nanorods system with elastic boundary conditions, how will the boundary restraining stiffness affect the longitudinal dynamic behavior of such multiple nanorod system? There is obviously a gap in the current literature on this aspect.

Motivated by the above existing limitation, an accurate series solution for the longitudinal vibration analysis of multiple nanorods system (MNRS) with general boundary and coupling conditions is established, in which an improved Fourier series method is employed for the axial vibration displacement expansion. Instead of solving the governing differential equation and boundary condition simultaneously, energy formulation is employed for the description of longitudinal dynamics of multiple nanorod system for the first time. Boundary smoothed auxiliary terms are introduced to the standard Fourier series with the aim to remove all the derivative discontinuity in the whole solving domain. System longitudinal modal characteristics can be obtained by solving a standard eigen-value matrix in conjunction with Rayleigh-Ritz procedure. Numerical examples are then presented to validate the proposed model and to study the influence of boundary restraints on the longitudinal vibration characteristics of MNRS. Finally, some concluding remarks are made.

2 Theoretical Formulations

2.1 Model Description

Consider the longitudinal vibration of elastically coupled multiple nanorod system (MNRS), as illustrated in Fig. 1, in which the axial restraining springs are introduced at both ends of each nanorod as well as the interface between each nanorod component. Then, any type of boundary and coupling conditions can be easily realized by setting the relevant stiffness coefficients accordingly. The coordinate systems used in this study are also illustrated, with the main geometrical and material parameters of MNRS. Longitudinal vibration displacement distribution is represented by $U(x, t)$.

Based on the vibration theory, when harmonic oscillation is assumed, the vibrating displacement function $U(x, t)$ can be further described as

$$U(x,t) = u(x)e^{j\omega t} \tag{1}$$

in which, $u(x)$ is the longitudinal vibration field function, and $e^{j\omega t}$ is the time factor for harmonic oscillation.

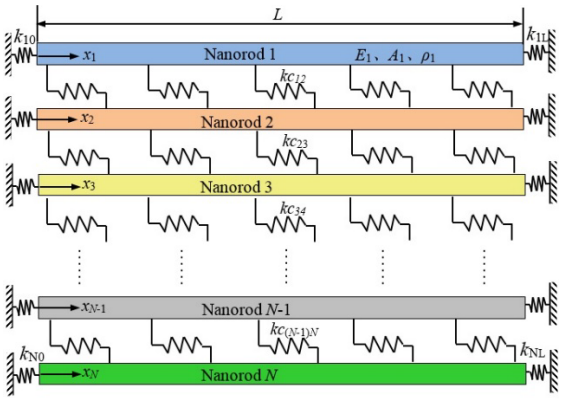

Figure 1: Elastically coupled MNRS with general boundary restraints

2.2 Nonlocal Rod Model Description

According to the nonlocal elasticity theory, one-dimensional nonlocal constitutive relationship of one nonlocal rod can be given as in Aydogdu (2009):

$$\sigma_x - (e_0 a)^2 \frac{\partial^2 \sigma_x}{\partial x^2} = E\varepsilon_x \tag{2}$$

where, σ_x is the axial stress, ε_x is the axial strain, $e_0 a$ is the scale coefficient representing the small-scale effect on the response of nanostructure, and E is the Young's modulus of the material.

The equation of motion for the axially vibrating rod can be written as

$$\frac{\partial N}{\partial x} = \rho A \frac{\partial^2 U}{\partial t^2} \tag{3}$$

here, ρ is the mass density, A is the area of the cross-section, and N is the axial force per unit length, which is defined by

$$N = \int_A \sigma_x dA \tag{4}$$

Integrating Eq. (2) over the cross-section area, one can get

$$N - (e_0 a)^2 \frac{\partial^2 N}{\partial x^2} = EA \frac{\partial u}{\partial x} \tag{5}$$

Then, by substituting Eq. (3) into Eq. (5), the axial force N cab be obtained as follows:

$$N = EA\frac{\partial u}{\partial x} + (e_0 a)^2 \frac{\partial}{\partial x}\left(\rho A \frac{\partial^2 u}{\partial t^2}\right) \tag{6}$$

Eq. (6) is the axial force expression for such nonlocal rod model, from which the potential energy can be further formulated. When $e_0 a$ is set to be zero, the above nonlocal rod model will be degenerated to the familiar classical rod model, which is then reduced to the governing equation of classical rod.

2.3 Energy Formulation and Its Series Solution

Based on the above nonlocal rod model, one can investigate its longitudinal vibration behavior by solving the partial differential governing equation and the boundary conditions, simultaneously. However, such approach will be too tedious when arbitrary number of MNRS are involved, especially with the complex boundary and coupling conditions. An equivalent way to describe the structural dynamics is the energy principle, for which the accurate solution can be derived when the sufficiently smoothed field admissible function is constructed. Furthermore, the complex coupling of multiple nanorod system can be treated in a unified pattern, and other attachments such as concentrated mass and spring elements can be easily introduced to the whole coupling system. For this reason, the multiple nanorod system with general boundary and coupling conditions will be described using the energy formulation. The corresponding Lagrangian function for the can be written as

$$L = V - T = \sum_{i=1}^{N} V_i + \sum_{i=1}^{N-1} V_{coupling}^{i,i+1} - \sum_{i=1}^{N} T_i \tag{7}$$

in which, V and T are the total potential energy and kinetic energy, respectively. V_i is the potential energy associated with the i^{th} nanorod member, $V_{coupling}^{i,i+1}$ is the potential energy stored in the coupling spring between the i^{th} and i+1$^{\text{th}}$ nanorods interface, and T_i is the kinetic energy of the i^{th} vibrating nanorod. The subscript i represents the i^{th} nanorod member.

For the i^{th} nanorod member with elastically restrained edges, the potential energy V_i is

$$\begin{aligned} V_i = {} & \frac{1}{2}\int_0^L \left[E_i A_i - \omega^2 \rho_i A_i (e_0 a)^2\right]\left(\frac{\partial U_i}{\partial x}\right)^2 dx \\ & + \frac{1}{2}k_{i0} U_i^2(x)\Big|_{x=0} + \frac{1}{2}k_{iL} U_i^2(x)\Big|_{x=L} \end{aligned} \tag{8}$$

where, $u(x)$ is the axial vibration displacement field function, k_0 and k_L are the stiffness coefficients at the ends x=0 and x=L, respectively.

The total kinetic energy of the i^{th} nanorod structure is

$$T_i = \frac{1}{2}\rho_i A_i \int_0^L \left[\frac{\partial U_i(x,t)}{\partial t}\right]^2 dx \tag{9}$$

here, ω is the radian frequency, ρ_i and A_i are respectively the mass density and cross section area of the i^{th} nanorod member.

The coupling potential energy between the nanorod interface can be written as

$$V_{coupling}^{i,i+1} = \frac{1}{2}\int_0^L \left[k_c^i (U_i - U_{i+1})^2\right] dx - (e_0 a)^2 \frac{1}{2}\int_0^L \left[k_c^i (U_i' - U_{i+1}')^2\right] dx \tag{10}$$

in which, k_c means the coupling spring stiffness between the i^{th} and i+1$^{\text{th}}$ nanorod member.

For the longitudinal vibration energy description of MNRS formulated above, it can be clearly seen that arbitrary number of nanorods and complex boundary conditions can be taken into account

through the modification of corresponding potential and kinetic energies as in Eqs. (7)-(10). Actually, even the non-uniform coupling stiffness distribution can be also treated, which will be very difficult by solving the governing equations. Making use of the system Lagrangian of Eq. (7), the solution can be obtained in conjunction with Rayleigh-Ritz procedure. When the sufficiently smoothed admissible function can be constructed in the whole solving region [0, L], the solution will be accurate enough and equivalent to that obtained by solving the differential equation and boundary conditions, simultaneously. In the structural dynamic community, Fourier series has been usually employed for the displacement expansion, especially for the classical boundary conditions, such as simply supported, free or clamped. However, the term-by-term differential operation of Fourier series will encounter the discontinuity at the end points, and its convergence and accuracy will be hard to guarantee for the case of non-ideal elastic boundary condition. For this reason, an improved version of Fourier series will be utilized for the displacement field expression under general boundary condition, in which the supplementary polynomials are introduced to the standard Fourier series to overcome all the discontinuities associated with the spatial derivative of displacement field function. In this work, the longitudinal vibration displacement function of each nanorod are invariantly expanded as

$$u(x) = \sum_{n=0}^{\infty} a_n \cos(\lambda_n x) + b_1\zeta_1(x) + b_2\zeta_2(x) \tag{11}$$

in which,

$$\zeta_1(x) = x\left(\frac{x}{L} - 1\right)^2, \qquad \zeta_2(x) = \frac{x^2}{L}\left(\frac{x}{L} - 1\right). \tag{12a, b}$$

It can be easily proven that the current constructed auxiliary functions can satisfy the displacement and its higher-order differentiation continuity requirement in the interval [0, L]. It should be noted that the choice of the supplementary functions is not unique, while the appropriate form will be helpful for simplifying the subsequent mathematical formulations.

Substituting the combined series expansion Eq. (11) into the elastically coupled MNRS Lagrangian Eqs. (7-10), minimizing it with respect to all the unknown coefficients and truncating the Fourier series into n=N, the system characteristic equation will obtain in matrix form as

$$\left(\mathbf{K} - \omega^2\mathbf{M}\right)\mathbf{A} = \mathbf{0} \tag{13}$$

where, **K** and **M** are the stiffness and mass matrices for the elastically connected multiple nanorod system, **A** is the unknown coefficient vector. By solving this standard eigen-value problem, all the associated modal characteristics, including natural frequency and mode shape, can be easily derived.

3 Numerical Results and Discussion

In this section, the above modelling framework is programmed in MATLAB environment. Several numerical results of elastically connected MNRS with arbitrary boundary conditions will be presented to demonstrate the effectiveness and advantage of the proposed model. As pointed out in the previous section, all the classical boundary conditions, such as free and clamped, can be easily obtained by setting the relevant spring stiffness coefficients into zero or infinity, accordingly. For the validation purpose, parameters in the simulation are chosen the same as those used in [23], namely L = 1 nm, ρA = 1 kg/nm, E = 1 nN and e_0a = 0-2 nm.

3.1 Double Nanorods with the Clamped-free and Clamped-Clamped Ends

As the first example, the double nanorods with the clamped-clamped and clamped-free boundary conditions will be considered. Spring stiffness coefficient k_c represents the coupling strength between these two nanorods. Tab. 1 tabulates the first four natural frequencies of one nanorod system with the coupling

spring k_c=0, which means these two nanorods are single and independent with each other. From Tab. 1, the current results agree well with those from the classical results and other approach in literature.

Table 1: Comparison of the four natural frequencies (GHz) of double nanorod system under C-C boundary condition with k_c = 0 N/nm

Mode	e_0a = 0 nm		e_0a = 1.0 nm		e_0a = 2.0 nm	
	Current	Classical	Current	Aydogdu, 2009	Current	Aydogdu, 2009
1	3.1415	3.1416	0.9529	0.9529	0.4938	0.4938
2	6.2831	6.2832	0.9876	0.9876	0.4984	0.4984
3	9.4246	9.4248	0.9944	0.9944	0.4993	0.4993
4	12.5661	12.5664	0.9968	0.9968	0.4996	0.4996

Tab. 2 and Tab. 3 present the results of first eight natural frequencies of DNRS under C-F boundary condition with the lower and higher couplings springs coefficients, namely k_c = 8 N/nm and k_c = 80 N/nm. From these two tables, the good agreement between the current results and those from other approaches can be observed repeatedly for different coupling strength and small-scale parameters. It is interesting to find that some of certain natural frequencies keep the same in Tab. 2 and Tab. 3, although the coupling strength is changed. To get a better understanding of this phenomenon, the first four mode shapes of DNRS are plotted in Figs. 2 and 3 for the coupling strength k_c = 8 N/nm and 80 N/nm, respectively. In each plot, it can be clearly seen that the mode shape exhibits the pair characteristics. For example, the spatial distribution of the first two modes are identical, while two types of phase relationship are observed, namely in the same and opposite phases. In this way, the "pair" can defined for such DNRS, which is denoted by the word "*p*" in the table. In each mode pair, the first mode shape amplitudes are identical, while the other ones are in different phase, and then the natural frequencies are also different. Through the comparison between Fig. 2 and Fig. 3, it can be found that the variation of coupling stiffness will not affect the first mode of each pair, for which the mode shapes for each nanorod are in the same phase, and then there is also no effect on the corresponding natural frequencies.

Table 2: Comparison of the first four pairs' natural frequencies (GHz) of double nanorod system under C-F boundary condition with *k*c = 8 N/nm

p	e_0a = 0 nm		e_0a = 0.5 nm		e_0a = 1.5 nm	
	Current	Erol H, 2004	Current	Karličić, 2015	Current	Karličić, 2015
1	1.5708	1.5708	1.2353	1.2353	0.6137	0.6137
	4.2974	4.2974	4.1864	4.1864	4.0468	4.0468
2	4.7123	4.7124	1.8411	1.8411	0.6601	0.6601
	6.1811	6.1812	4.4033	4.4033	4.0541	4.0541
3	7.8539	7.8540	1.9381	1.9381	0.6643	0.6643
	8.8138	8.8139	4.4448	4.4448	4.0548	4.0548
4	10.9955	10.9956	1.9677	1.9677	0.6654	0.6654
	11.7004	11.7005	4.4578	4.4578	4.0550	4.0550

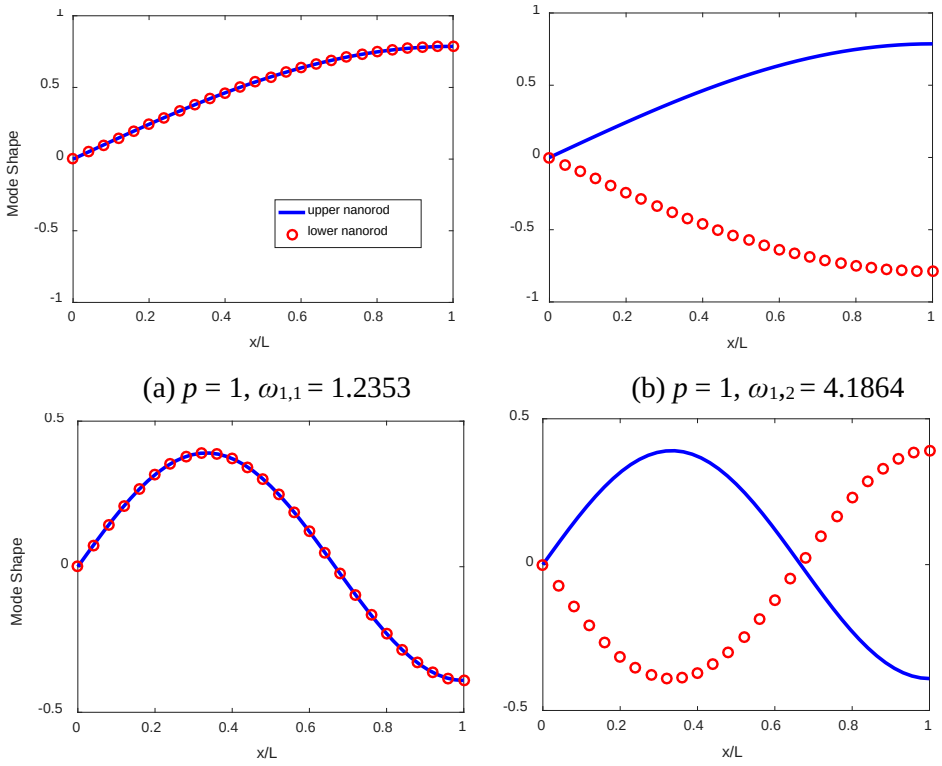

(a) p = 1, $\omega_{1,1}$ = 1.2353 (b) p = 1, $\omega_{1,2}$ = 4.1864

(c) p = 2, $\omega_{2,1}$ = 1.8411 (d) p = 2, $\omega_{2,2}$ = 4.4033

Figure 2: The first two pairs' mode shapes of double nanorod system under C-F boundary condition with k_c = 8 N/nm and e_0a = 0.5 nm

Table 3: Comparison of the first four pairs' natural frequencies (GHz) of double nanorod system under C-F boundary condition with kc = 80 N/nm

p	e_0a = 0 nm		e_0a = 0.5 nm		e_0a = 1.5 nm	
	Current	Erol H, 2004	Current	Karličić, 2015	Current	Karličić, 2015
1	1.5708	1.5708	1.2353	1.2353	0.6137	0.6137
	12.7463	12.7463	12.7093	12.7093	12.6640	12.6640
2	4.7123	4.7124	1.8411	1.8411	0.6601	0.6601
	13.4984	13.4984	12.7824	12.7824	12.6663	12.6663
3	7.8539	7.8540	1.9381	1.9381	0.6643	0.6643
	14.8890	14.8891	12.7967	12.7967	12.6665	12.6665
4	10.9955	10.9956	1.9677	1.9677	0.6654	0.6654
	16.7601	16.7602	12.8012	12.8012	12.6666	12.6666

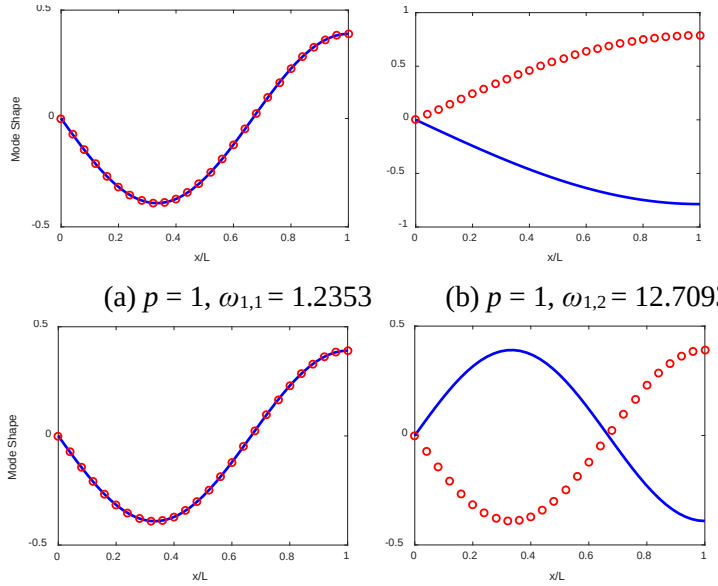

(a) p = 1, $\omega_{1,1}$ = 1.2353 (b) p = 1, $\omega_{1,2}$ = 12.7093

(c) p = 2, $\omega_{2,1}$ = 1.8411 (d) p = 2, $\omega_{2,2}$ = 12.7824

Figure 3: The first two pairs' mode shapes of double nanorod system under C-F boundary condition with k_c = 80 N/nm and e_0a = 0.5 nm

3.2 Effect of the Elastic Boundary Restraints for DNRS

Here, the elastic boundary condition of double nanorods system will be taken into account at the coupling spring stiffness kc = 8 and 80 N/nm. Influence of elastic boundary restraint on the first mode frequency of fundamental pair are calculated for two cases of coupling strength and presented in Fig. 4. In the numerical simulation, the upper nanorods is elastically restrained at each end, while the lower one is specified as the C-F boundary condition. In this figure, k_{10} and k_{1L} mean the boundary spring coefficients of upper rod at x = 0 and x = L, respectively. In general, the similar influence trends as in Section 3.1 can be seen for the fundamental frequency of DNRS for these two coupling stiffness coefficients through the comparing the value of (a) and (b) in Fig. 4. While the small difference between these two can be found in the right-up zone of the boundary restraining stiffness, which means the different trend can be observed when the upper nanorods tends to be set as the F-C boundary condition. Then the anti-symmetric boundary restraints will be obtained for these two nanorods, and the coupling strength will affect the first mode of this fundamental "pair" to some extent.

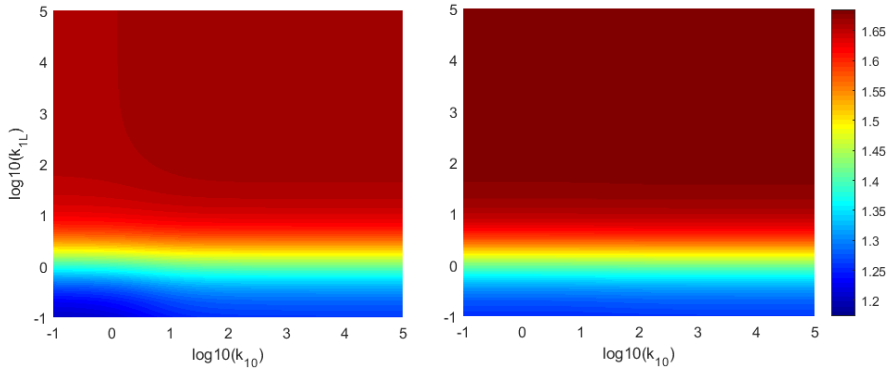

(a) (b)

Figure 4: Influence of elastic restraining stiffness of upper rod on the fundamental frequency, with the lower rod under C-F boundary condition and e_0a = 0.5. (a) k_c = 8 N/nm; (b) k_c = 80 N/nm

Right now, let us consider the boundary conditions for both nanorods are elastic boundary restraints, in which k_1 and k_2 are used to represent the elastic coefficients for the upper and lower nanorods, and for each one the right and left ends have the same restraining stiffness. Influence of boundary restraints on the second longitudinal modes of fundamental pair is calculated and plotted in Fig. 5. From this figure, it can be seen that the variation of boundary restraining stiffness of nanorods will have a significant effect on the frequencies of the second frequency of fundamental pair of DNRS. However, variation of frequency parameter is not uniform, and there exists a sensitive zone of stiffness coefficients affecting the frequency parameters and the sensitive zone of elastic stiffness is symmetric due to such configuration of boundary restraints. When increasing the small-scale parameter, it can be observed that there is an overall decrease of natural frequency, since the increase of nonlocal parameter will make the nanorod much softer in an overall pattern.

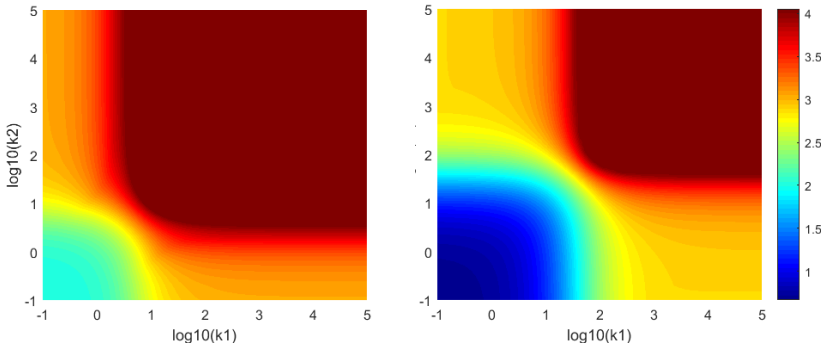

(a) (b)

Figure 5: Influence of the upper and lower boundary restraining stiffness on the second frequency of fundamental pair of DNRS with the coupling strength as $k_c = 8$ N/nm. (a) $e_0a = 0.5$; (b) $e_0a = 1.5$

With aim to illustrate the combined effects of boundary restraining stiffness and the coupling strength on such frequency of DNRS with different small-scale parameters, the simulation is recalculated while the coupling stiffness set as 80 N/nm. The results are plotted in Fig. 6. It can be seen that the influence trends keep similar to those presented in Fig. 5, while the increase of coupling strength cause the increase of frequencies as expected. Between these two cases of small-scales parameters, the larger nonlocal parameter will cause the decrease of resonant frequency at certain extents while keeping the symmetric trends of boundary restraining stiffness sensitive zone.

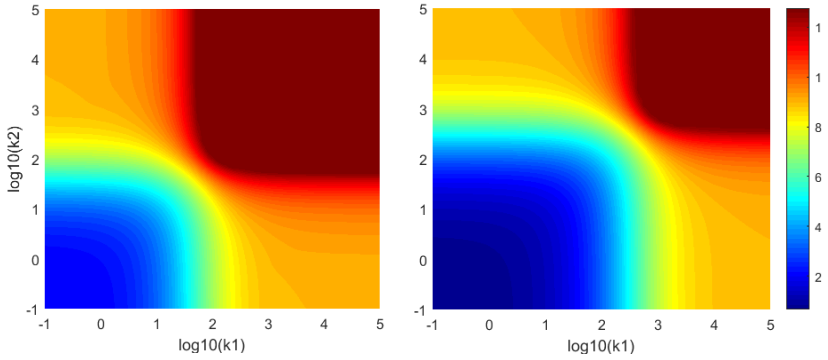

(a) (b)

Figure 6: Influence of the upper and lower boundary restraining stiffness on the second frequency of fundamental pair of DNRS with the coupling strength as $k_c = 80$ N/nm. (a) $e_0a = 0.5$; (b) $e_0a = 1.5$

3.3 Results of MNRS with Different Boundary Conditions

Finally, let us move our attention to the case of multiple nanorods system. As pointed out in the theoretical section, the current modeling framework can treat the multiple coupling between the nanorods much easily. One just needs to include the potential and kinetic energy components of additional nanorods into the total Lagrangian Eq. (7), which can be readily realized in the current sub-domain approach. Similar to the above double nanorods system, the "triple" concept can also used for the presentation of the longitudinal modes of MNRS. Natural frequencies for the first three triple of MNRS under C-F boundary condition with $kc_{12} = kc_{23} = 8$ N/nm are computed and tabulated in Tab. 4. Comparing with the results for DNRS in Tab. 2, it can be seen that the first mode of each triple is the same as those corresponding pair. To understand the modal behavior of three nanorods system much better, the mode shape for the first three triple are also plotted in Fig. 7. It can be observed that for such identical coupling strength these three nanorods in the first mode of each triple vibrate in the same phase with the identical amplitude, which means that these three nanorods will behave like a single one. This phenomenon may be defined as the invariable characteristics of MNRS. Similarly, with the increase of nonlocal parameter, a uniform decrease trends of natural frequency can be observed, and the convergence property can be also seen for such nonlocal nanorods system, for which further increase of nonlocal parameter will not cause the variation of natural frequencies any more. Another interesting modal behavior of such three nanorods system can be observed for the second mode of each triple, and there is no vibrating deformation for the medium nanorod due to such symmetric coupling configuration for its upper and lower nanorods.

Table 4: Natural frequencies (GHz) of the first three triple of three nanorods system under C-F boundary condition with $k_{c12} = k_{c23} = 8$ N/nm

t	e_0a = 0.5 nm	e_0a = 1.0 nm	e_0a = 1.5 nm	e_0a = 2 nm
	1.2353	0.8436	0.6137	0.4764
1	3.0864	2.9515	2.8942	2.8683
	5.0523	4.9711	4.9373	4.9221
	1.8411	0.9782	0.6601	0.4972
2	3.3748	2.9928	2.9044	2.8718
	5.2335	4.9957	4.9433	4.9241
	1.9381	0.9920	0.6643	0.4990
3	3.4288	2.9973	2.9054	2.8721
	5.2684	4.9984	4.9438	4.9243

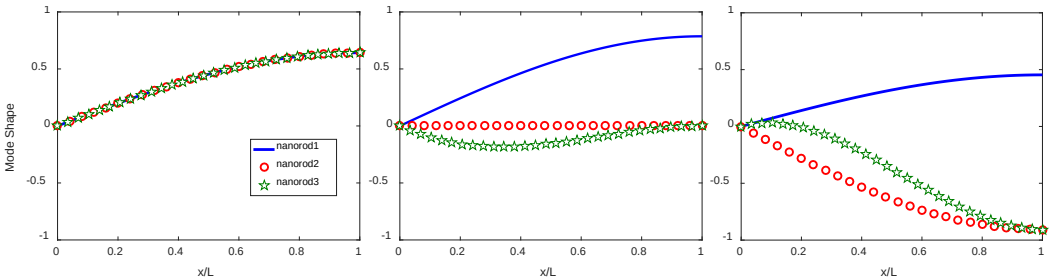

(a) $t = 1$, $\omega_{1,1} = 1.2353$ (b) $t = 1$, $\omega_{1,2} = 3.0864$ (c) $t = 1$, $\omega_{1,3} = 5.0523$

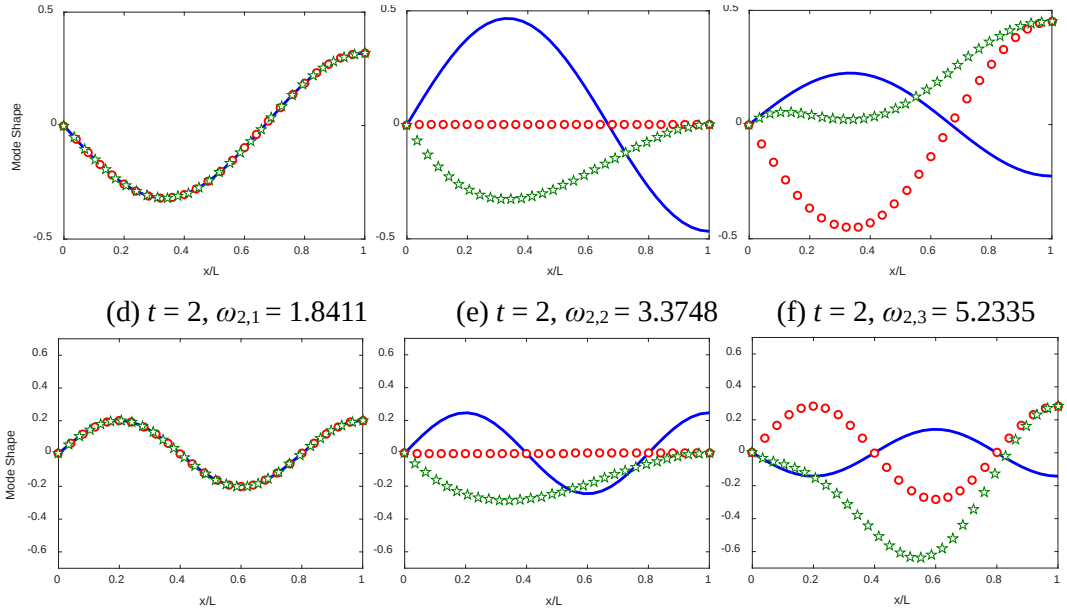

(d) t = 2, $\omega_{2,1}$ = 1.8411 (e) t = 2, $\omega_{2,2}$ = 3.3748 (f) t = 2, $\omega_{2,3}$ = 5.2335

(g) t = 3, $\omega_{3,1}$ = 1.9381 (h) t = 3, $\omega_{3,2}$ = 3.4288 (i) t = 3, $\omega_{3,3}$ = 5.2684

Figure 7: The first three triples' mode shapes of three nanorod system under C-F boundary condition with $kc_{12} = kc_{23} = 8$ N/nm and $e_0a = 0.5$ nm

Finally, a non-symmetric coupling case is considered, namely $kc_{12} = 2$ N/nm and $kc_{23} = 8$ N/nm, with other parameters kept the same. Then, this is recalculated and the results are presented in Tab. 5. Since the first mode of fundament triple behaves like three separate single nanorods with the same phase and amplitude, then here it can be seen again the natural frequency for this mode is still the same, namely the invariable characteristics still exists. With the aim to have a look at the second of each triple, the corresponding modes shapes are plotted in Fig. 8, it can be found that the displacement of nanorod 2 is not zero for this non-symmetric coupling configuration.

Table 5: Natural frequencies (GHz) of the first three triple of three nanorods system under C-F boundary condition with $kc_{12} = 2$ N/nm and $kc_{23} = 8$ N/nm

r	e_0a = 0.5 nm	e_0a = 1.0 nm	e_0a = 1.5 nm	e_0a = 2 nm
	1.2353	0.8436	0.6137	0.4764
1	2.0537	1.7320	1.5635	1.5000
	3.1623	2.6458	2.5386	2.5000
	1.8411	0.9782	0.6601	0.4972
2	2.3921	1.7320	1.5635	1.5000
	3.1624	2.6458	2.5386	2.5000
	1.9381	0.9920	0.6643	0.4990
3	2.4323	1.7321	1.5635	1.5000
	3.1624	2.6458	2.5386	2.5000

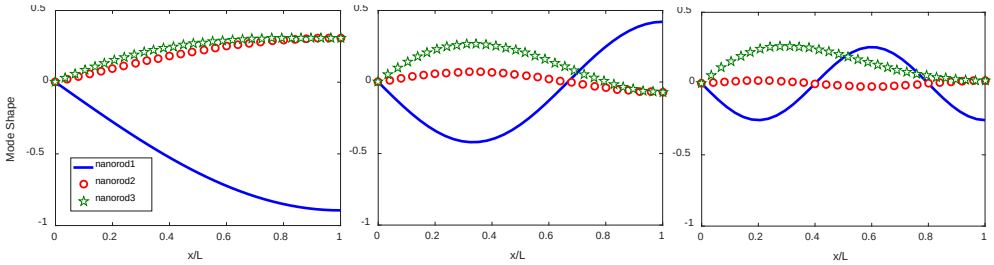

(a) $r = 1$, $\omega_{1,2} = 2.0537$ (b) $r = 2$, $\omega_{2,2} = 2.3921$ (c) $r = 3$, $\omega_{3,2} = 2.4323$

Figure 8: The second mode of each triple of three nanorod system under C-F boundary condition with kc_{12} = 2 N/nm, kc_{23} = 8 N/nm and e_0a = 0.5 nm

4 Conclusion

In this paper, an accurate solution for the longitudinal vibration analysis of multiple nanorods system (MNRS) with general boundary and coupling conditions has been established based on nonlocal elasticity theory. Energy formulation for the longitudinal vibration of MRNS is derived for the first time. Longitudinal displacement of nanorod is constructed as an improved Fourier series with auxiliary polynomials in order to make the differential sufficiently smooth in the whole solving region [0, L]. Dynamic coupling between nanorods are implemented through the introduction of elastic springs distributed on each interface, which can be easily taken into account through the inclusion of potential energy term in system Lagrangian. In conjunction with Rayleigh-Ritz procedure, all the modal characteristics can be obtained by solving a standard eigen-value matrix.

Several numerical examples are presented to demonstrate the correctness and reliability of the proposed model through comparing with the data calculated from other approach in literature. Excellent agreement has been repeatedly observed for the longitudinal vibration analysis of DNRS with various boundary conditions. Influence of boundary restraint, coupling stiffness and small-scale parameter are also discussed and addressed. For the elastic boundary restraint, there exists a sensitive range in which variation of spring stiffness will affect the natural frequencies greatly and will move as the change of small-scale parameter as well as coupling springs stiffness. The pair and triple phenomenon have been observed from the mode shape presentation, and the invariable characteristics exists for such MNRS. The current model treats the boundary and coupling conditions in a unified pattern, any modification of system parameters will not cause the reformulation of theoretical description. This work can also provide an efficient tool for examining the dynamic behavior of MNRS, especially with complex boundary and coupling conditions.

Acknowledgement: This work was supported by the Fok Ying Tung Education Foundation (Grant No. 161049).

References

1. Deotare, P. B., Mccutcheon, M. W., Frank, I. W., Khan, M., Loncar, M. (2009). Coupled photonic crystal nanobeam cavities. *Applied Physics Letters, 95(3),* 207.
2. Wen, J. G., Lao, J. Y., Wang, D. Z., Kyaw, T. M., Foo, Y. L. et al. (2003). Self-assembly of semiconducting oxide nanowires, nanorods, and nanoribbons. *Chemical Physics Letters, 372,* 717-722.
3. Lin, Q., Rosenberg, J., Chang, D., Camacho, R., Eichenfield, M. et al. (2010). Coherent mixing of mechanical excitations in nano-optomechanical structures. *Nature Photonics, 4(4),* 236-242.
4. Wang, C. M., Duan, W. H. (2008). Free vibration of nanorings/arches based on nonlocal elasticity. *Journal of Applied Physics, 104(1), 014303.*
5. Heireche, H., Tounsi, A., Benzair, A., Maachou, M., Bedia, A. (2008). Sound wave propagation in single-walled carbon nanotubes using nonlocal elasticity. *Physica E, 40,* 2791-2799.

6. Yang, J., Ke, L. L., Kitipornchai, S. (2010). Nonlinear free vibration of single-walled carbon nanotubes using nonlocal Timoshenko beam theory. *Physica E, 42,* 1727-1735.
7. Murmu, T., Pradhan, S. C. (2009). Vibration analysis of nanoplates under uniaxial prestressed conditions via nonlocal elasticity. *Journal of Applied Physics, 106,* 104301.
8. Phadikar, J. K., Pradhan, S. C. (2010). Variational formulation and finite element analysis for nonlocal elastic nanobeams and nanoplates. *Computational Materials Science, 49,* 492-499.
9. Eringen, A. C. (1983). On differential equations of nonlocal elasticity and solutions of screw dislocation and surface waves. *Journal of Applied Physics, 54,* 4703-4710.
10. Lu, P. (2007). Dynamic analysis of axially prestressed micro/nanobeam structures based on nonlocal beam theory. *Journal of Applied Physics, 101,* 073504.
11. Reddy, J. N. (2007). Nonlocal theories for bending, buckling and vibration of beams. *International Journal of Engineering Science, 45,* 288-307.
12. Aydogdu, M. (2009). A general nonlocal beam theory: its application to nanobeam bending, buckling and vibration. *Physica E, 41,* 1651-1655.
13. Wang, C. M., Zhang, Y. Y., Ramesh, S. S., Kitipornchai, S. (2006). Buckling analysis of micro-and nano-rods/tubes based on nonlocal Timoshenko beam theory. *Journal of Physics D: Applied Physics, 39,* 3904-3909.
14. Gul, U., Aydogdu, M. (2018). Structural modelling of nanorods and nanobeams using doublet mechanics theory. *International Journal of Mechanics and Materials in Design, 14,* 195-212.
15. Peddieson, J., Buchanan, G. R., McNitt, R. P. (2003). Application of nonlocal continuum models to nanotechnology. *International Journal of Engineering Science, 41,* 305-312.
16. Ansari, R., Rouhi, H. (2012). Analytical treatment of the free vibration of single-walled carbon nanotubes based on the nonlocal Flugge shell theory. *Journal of Engineering Materials and Technology, 134,* 011008.
17. Lei, Y., Adhikari, S., Friswell, M. I. (2013). Vibration of nonlocal Kelvin-Voigt viscoelastic damped Timoshenko beams. *International Journal of Engineering Science, 66,* 1-13.
18. Danesh, M., Farajpour, A., Mohammadi, M. (2012). Axial vibration analysis of a tapered nanorod based on nonlocal elasticity theory and differential quadrature method. *Mechanics Research Communications, 39,* 23-27.
19. Aydogdu, M. (2009). Axial vibration of the nanorods with the nonlocal continuum rod model. *Physica E, 41,* 861-864.
20. Kiani, K. (2010). Free longitudinal vibration of tapered nanowires in the context of nonlocal continuum theory via a perturbation technique. *Physica E, 43,* 387-397.
21. Guo, S. Q., Yang, S. P. (2012). Axial vibration analysis of nanocones based on nonlocal elasticity theory. *Acta Mechanica Sinica, 28,* 801-807.
22. Xu, D., Du, J., Liu, Z. (2016). Longitudinal vibration analysis of nonlocal nanorods with elastic end restraints by an improved Fourier series method. *Noise Control Engineering Journal, 64,* 766-778.
23. Murmu, T., Adhikari, S. (2010). Nonlocal effects in the longitudinal vibration of double-nanorod systems. *Physica E, 43,* 415-422.
24. Karličić, D., Cajić, M., Murmu, T., Adhikari, S. (2015). Nonlocal longitudinal vibration of viscoelastic coupled double-nanorod systems. *European Journal of Mechanics-A/Solids, 49,* 183-196.
25. Erol, H., Gürgöze, M. (2004). Longitudinal vibrations of a double-rod system coupled by springs and dampers. *Journal of Sound and Vibration, 276,* 419-430.
26. Muthukumaran, P., Bhat, R. B., Stiharu, I. (1999). Boundary conditioning technique for structural tuning. *Journal of Sound and Vibration, 220,* 847-859.
27. Kobrinsky, M. J., Deutsch, E. R., Senturia, S. D. (2000). Effect of support compliance and residual stress on the shape of doubly supported surface-micromachined beams. *Journal of Microelectromechanical Systems, 9,* 361-369.
28. Alkharabsheh, S. A., Younis, M. I. (2013). Dynamics of MEMS arches of flexible supports. *Journal of Microelectromechanical Systems, 22,* 216-224.
29. Zhong, Z. Y., Zhou, J. P., Zhang, H. L., Zhang, T. (2016). Effect of the equivalent stiffness of flexible supports on the MEMS cantilever-based sensors. *Computers & Structures, 169,* 101-111.